J Toxicol Pathol 2023; 36: 159–169

Original Article

Effects of cyclophosphamide on rat placental development

Satoshi Furukawa[1*], Naho Tsuji[2], Seigo Hayashi[3], Yusuke Kuroda[3], Masayuki Kimura[3], Chisato Kojima[3], and Kazuya Takeuchi[3]

[1] Planning and Development Department, Nissan Chemical Corporation, 2-5-1 Nihonbashi, Chuo-ku, Tokyo 103-6119, Japan
[2] Planning and Development, Agricultural Chemical Division, Nissan Chemical Corporation, 2-5-1 Nihonbashi, Chuo-ku, Tokyo 103-6119, Japan
[3] Biological Research Laboratories, Nissan Chemical Corporation, 1470 Shiraoka, Shiraoka-shi, Saitama 349-0294, Japan

Abstract: We examined the morphological effects of cyclophosphamide (CPA) on placental development in pregnant rats. CPA was administered as a single dose to pregnant rats intraperitoneally at 0 mg/kg (the control group), 25 mg/kg on gestation day (GD) 12 (the CPA GD 12-treated group), and 25 mg/kg on GD 14 (the CPA GD 14-treated group). The fetal and placental weight decreased in the CPA-treated groups, complete fetal resorption from GD 17 onwards in the CPA GD 12-treated group, and external malformations in the CPA GD 14-treated group. Histopathologically, CPA induced apoptosis and/or cell proliferation inhibition in each part of the placenta. In the labyrinth zone, syncytiotrophoblasts were selectively reduced, resulting in a small placenta. In the basal zone, the number of spongiotrophoblasts was reduced, resulting in hypoplasia of glycogen cell islands. In addition, a small number of interstitial trophoblasts invaded the metrial gland from the basal zone on GD 15. The severity of these lesions was higher in the CPA GD 12-treated group than in the CPA GD 14-treated group. In the metrial gland, although the number of uterine natural killer cells was reduced, metrial gland development was not affected. (DOI: 10.1293/tox.2022-0144; J Toxicol Pathol 2023; 36: 159–169)

Key words: apoptosis, cyclophosphamide, rat, small placenta, syncytiotrophoblast

Introduction

The placenta is a temporary organ that plays a pivotal role in fetal growth, including the mediation of maternal immune tolerance, hormone production, nutrient uptake, waste elimination, and gas exchange[1, 2]. The placenta consists of the fetal (labyrinth zone, basal zone, and yolk sac) and maternal (decidua and metrial gland)[2] parts. Because the placenta grows rapidly for a short period, each part has high cell proliferation activity. However, the cell proliferation patterns among these parts differ during normal placental development. Therefore, the placenta is highly sensitive to antineoplastic drugs that are involved in cell proliferation inhibition and apoptosis, and these drug-induced placental lesions depend on the exposure period, similar to the fetal sensitive period of teratogenicity[3, 4].

Cyclophosphamide (CPA) is an alkylating antineoplastic and immunosuppressive agent used as a therapy for solid tumors, Hodgkin's disease, and non-neoplastic conditions such as rheumatic arthritis. The antineoplastic effect of CPA is due to its metabolite phosphoramide mustard[5], which reacts with purine bases in DNA to form adducts and triggers apoptosis[6]. Phosphoramide mustard-induced apoptosis plays an important role in CPA teratogenesis[7]. CPA is known to induce a variety of malformations in the brain, limbs, face, skeleton, and tail of many animal species, including mice, rats, rabbits, monkeys, humans, and chicks[8, 9]. In addition, CPA is known to induce placental toxicity in rats and mice[10, 11]. However, there have been no reports describing the detailed sequential histopathological changes in the placenta of rats exposed to CPA. In the present study, we administered a single intraperitoneal dose of CPA to pregnant rats on gestation day (GD) 12 or 14 and performed a histopathological examination of the placentas on GDs 13, 15, 17, and 21 to elucidate the sequential morphological effects of CPA on placental development and compare the placental lesions caused by the different timing of CPA administration.

Received: 10 January 2023, Accepted: 16 February 2023
Published online in J-STAGE: 24 March 2023
*Corresponding author: S Furukawa
(e-mail: furukawa@nissanchem.co.jp)

Materials and Methods

Animals

Pregnant specific pathogen-free Wistar Hannover rats (BrlHan: WIST@Jcl (GALAS), CLEA Japan, Tokyo, Japan) were purchased at approximately 11–12 weeks of age. The animals were single-housed in plastic cages on softwood

chip bedding in an air-conditioned room (22 ± 2°C, 55 ± 10% humidity; 12 h/day light cycle). Food (CRF-1; Oriental Yeast Co., Ltd., Tokyo, Japan) and water were provided *ad libitum*.

Experimental design

Forty-four pregnant rats (GD 7) were randomly allocated to three groups of 12 or 16 rats each (Table 1). GD 0 was designated as the day on which the vaginal plug was identified. CPA (Tokyo Chemical Industries, Ltd., Tokyo, Japan) was dissolved in saline solution. CPA was then administered as a single intraperitoneal dose to the groups at doses of 0 mg/kg with saline on GD 12 (the control group), 25 mg/kg on GD 12 (the CPA GD 12-treated group), and 25 mg/kg on GD 14 (the CPA GD 14-treated group), with a volume of 0.5 mL/100 g body weight. The CPA dose was selected as 25 mg/kg because CPA treatment of pregnant rats at 10–30 mg/kg on GD 13.5 has been reported to have teratogenic effects[12]. The CPA dosing day was selected as GD 12 or 14, because embryonic death on GD 13 was noted using a single intraperitoneal administration of CPA at 25 mg/kg on GD 10 in the pilot study. All treatments were conducted between 9 a.m. and 11 a.m. Maternal body weight was recorded from GD 7 to GD 21. Dams (number of animals = 4/each time point/group) were sampled on GDs 13, 15, 17, and 21. The dams were euthanized by exsanguination under isoflurane anesthesia and subsequently necropsied. All fetuses were removed from the placenta. A third of the placentas were separated between the basal zone and decidua basalis and removed from the uterine wall. The fetuses and removed placentas were weighed and the individual fetal-placental weight ratios were calculated. The fetuses were macroscopically examined for external malformations on GDs 17 and 21. According to the criteria for intrauterine growth restriction (IUGR) evaluation, fetuses were defined as having IUGR if their weight was less than −2 standard deviations (SD) below the mean fetal weights in the control group on each GD[13], which was <0.058 g on GD 13, <0.213 g on GD 15, <0.714 g on GD 17, and <4.430 g on GD 21 in the present study. The IUGR rate (i.e., the actual number of fetuses exhibiting IUGR as a percentage of the total number of fetuses) was calculated. All fetal and placental samples were fixed in 10% neutral-buffered formalin. This study was conducted according to the Guidelines for Animal Experimentation, the Biological Research Laboratory, Nissan Chemical Corporation, and the statement regarding sedation, anesthesia, and euthanasia in a rodent fetus and newborn (2015) in the Japanese College of Laboratory Animal Medicine.

Histopathological examination

Four placentas, randomly selected for each dam, were embedded in one paraffin block, and 4 μm thick sections were routinely stained with hematoxylin and eosin for histopathological examination. The thicknesses of the labyrinth zone, basal zone, decidua basalis, and metrial gland close to the central portion of the placenta were measured once per placenta using an image analyzer (WinROOF, Mitani Co., Tokyo, Japan). The placentas were subjected to immunohistochemical staining of phospho-histone H3 (Ser10; Cell Signaling Technology, Boston, MA, USA) for cell proliferation evaluation, glucose transporter 1 (GLUT1, Abcam, Cambridge, UK), perforin (Torrey Pines Biolabs, Secaucus, NJ, USA) for uterine natural killer (uNK) cell detection, and *in situ* TdT-mediated dUTP nick end labeling (TUNEL; In Situ Cell Death Detection Kit, POD, Roche Applied Science, Penzberg, Germany) for apoptosis evaluation[14]. With the aid of the image analyzer, the numbers of phospho-histone H3-positive cells and TUNEL-positive cells in the labyrinth zone, basal zone, metrial gland, and yolk sac were counted in 20 sections per placenta using light microscopy with a 40

Table 1. Effects of Cyclophosphamide on the Fetus and Placenta

Autopsy	Group	No. of dams	Mean No. of live fetuses[a)]	Fetal mortality (%)[a)]	Fetus weight (g)[a)]	Placenta weight (g)[a)]	Fetus / Placenta (g/g)[a)]	IUGR rate (%)	External malformation rate (%)[a]
GD13	Control	4	12.3 ± 1.0	0.0 ± 0.0	0.07 ± 0.00	0.11 ± 0.01	0.61 ± 0.05	4.1	ND
	CPA GD12	4	12.5 ± 3.5	17.9 ± 16.6	0.05 ± 0.00 **	0.11 ± 0.01	0.42 ± 0.04 **	98.0 ++	ND
GD15	Control	4	13.8 ± 2.6	3.9 ± 4.7	0.26 ± 0.02	0.19 ± 0.01	1.37 ± 0.12	3.6	ND
	CPA GD12	4	4.3 ± 1.7 **	67.3 ± 13.9 **	0.14 ± 0.02 **	0.12 ± 0.02 **	1.25 ± 0.47	100.0 ++	ND
	CPA GD14	4	11.8 ± 1.0	4.0 ± 4.6	0.24 ± 0.01	0.20 ± 0.01	1.19 ± 0.07	8.7	ND
GD17	Control	4	13.5 ± 1.3	0.0 ± 0.0	0.78 ± 0.02	0.27 ± 0.01	3.01 ± 0.15	7.3	0.0
	CPA GD12	4	0.0 ± 0.0 **	100.0 ± 0.0 **	ND	ND	ND	ND	ND
	CPA GD14	4	12.8 ± 1.5	4.8 ± 6.0	0.43 ± 0.02 **	0.23 ± 0.02 *	1.89 ± 0.04 **	100.0 ++	100.0 ++
GD21	Control	4	13.8 ± 0.5	3.5 ± 4.0	5.01 ± 0.23	0.40 ± 0.08	12.72 ± 1.73	5.5	0.0
	CPA GD12	4	0.0 ± 0.0 **	100.0 ± 0.0 **	ND	ND	ND	ND	ND
	CPA GD14	4	14.3 ± 1.0	0.0 ± 0.0	2.19 ± 0.21 **	0.27 ± 0.01 *	8.11 ± 1.10 **	100.0 ++	100.0 ++

Mean ± SD.

a) Mean of individual litter values.

*, ** Significantly different from control at $p<0.05$, <0.01, respectively (Student's t-test/Aspin-Welch's t-test/Dunnett's test).

++ Significantly different from control at $p<0.01$ (Fisher exact test).

IUGR: intrauterine growth restriction; ND: not done.

× objective. There was no evaluation of the fetal parts of the placenta on GDs 17 and 21 in the CPA GD 12-treated group due to fetal death. The number of perforin-positive cells per unit area around the spiral arteries in the metrial gland was counted in five sections per placenta using light microscopy with a 20× objective.

Statistical analysis

The means and SDs of individual litter values were calculated (Pharmaco Basic, Scientist Press Co. Ltd., Tokyo, Japan). For comparisons between two groups, either the Student's t-test for homoscedastic data or the Aspin–Welch's t-test for non-homoscedastic data was performed after the F test. The Dunnett's multiple comparison test was performed to compare three groups. The Fisher's exact test was used to determine the incidence of IUGR and external malformations. The level of significance was set at $p<0.05$ and $p<0.01$.

Results

Effects on dams

The body weight gain (%) of dams (based on the body weight on GD 7 as 100%) decreased from GD 16 onwards in the CPA GD 12-treated group and from GD 17 onwards in the CPA GD 14-treated group, compared to the control group (Fig. 1). The marked reduction in dam body weight gain in the CPA GD 12-treated group was caused by fetal death. In all groups, no maternal mortality or clinical signs were observed in any dams during the experimental period.

Effects on embryos/fetuses and placentas

The effects of CPA administration on embryos/fetuses and placentas are shown in Table 1. In the CPA GD 12-treated group, fetal mortality increased from GD 13, and complete fetal resorption was observed from GD 17 onwards in all dams. There were decreases in fetal weight on GDs 13 and 15, placental weight on GD 15, and fetal-placental weight ratio on GD 13, and an increase in the incidence of IUGR on GDs 13 and 15. In the CPA GD 14-treated group, no effects on fetal mortality were observed during the experimental period. However, there were decreases in fetal weight, placental weight, and the fetal-placental weight ratio, and an increase in the incidence of IUGR on GDs 17 and 21. Macroscopically, the placentas on GDs 17 and 21 showed scattered map-like white spots with an enlarged white peripheral rim (Fig. 2). In the fetal external examination, all fetuses showed external malformations on GDs 17 and 21: dwarfism, craniofacial anomaly, cystic edema, or omphalocele on GD 17 (Fig. 2); exencephaly, exophthalmia, open eyes, misshapen snout, low-set ears, microtia, multiple focal absent skin, or umbilical hernia on GD 21 (Fig. 2). These malformations were identical to previous reports of CPA-exposed rats[9] and were probably induced by the direct effects of CPA.

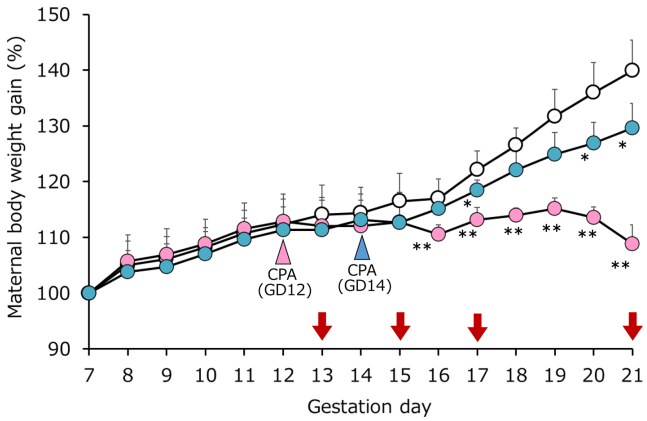

Fig. 1. Maternal body weight changes. *, ** Significantly different from control at $p<0.05$ and $p<0.01$, respectively (Dunnett's test). Error bar: standard deviations. White, control group; pink, cyclophosphamide (CPA) gestation day (GD) 12-treated group; blue, CPA GD 14-treated group. Arrow head, administration; Arrow, autopsy.

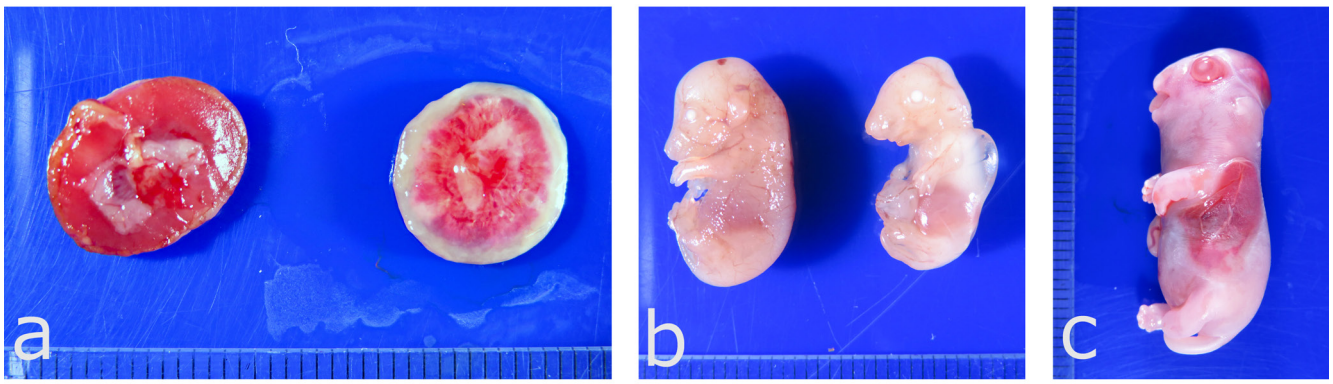

Fig. 2. Gross appearance of the placenta and fetus. a. Gross appearance of placentas on gestation day (GD) 21. Map-like white spots with enlarged white peripheral rim in the cyclophosphamide (CPA) GD 14-treated group. Left, control group; right, CPA GD 14-treated group. b. Gross appearance of fetuses on GD 17. Dwarfism, craniofacial anomaly, cystic edema, and umbilical hernia in the CPA GD 14-treated group. Left, control group; right, CPA GD 14-treated group. c. Gross appearance of fetuses on GD 21. Exencephaly, exophthalmia, open eyes, misshapen snout, low set ears, microtia, multiple focal absent skin, and umbilical hernia in the CPA GD 14-treated group.

Histopathological observations

Labyrinth zone

The thickness of the labyrinth zone decreased from GD 15 onwards, resulting in a small placenta in the CPA-treated groups (Figs. 3 and 4a). In the CPA-treated groups, apoptosis, characterized by pyknosis or karyorrhexis, phagocytosis, cell debris, and positive staining by the TUNEL method, increased in the trophoblastic septa (Fig. 4b). The number of TUNEL-positive cells increased on GDs 13 and 15 in the CPA GD 12-treated group and from GD 15 onwards in the CPA GD 14-treated group (Fig. 5). The small trophoblasts considered syncytiotrophoblasts, were selectively reduced, while the trophoblastic septa were partially thickened with a remarkable presence of large trophoblasts considered cytotrophoblasts, from GD 15 onwards (Fig. 4c). A thickened chorionic plate, calcification in the trophoblastic septa, and thrombosis in the maternal sinusoids were observed in some placentas (Fig. 4d). In the CPA GD 12-treated group, after GD 17 when the fetuses died, hemorrhages, thrombosis, necrosis of the trophoblastic septa, cystic dilatation of the maternal sinusoid, and chorionic plate thickening resulted in the disruption and regression of the labyrinth zone (Fig. 4a). In the GLUT1 immunohistochemistry, two proximate GLUT1-positive lines were detected on the maternal sinusoid side and fetal vessel side in the trophoblastic septa in the control group. Multiple clumps of small syncytiotrophoblasts surrounded by GLUT1 lines were observed in the trophoblastic septa on GD 13, and the clump size gradually decreased from GD 15 onwards (Fig. 4e). In the CPA-treated groups, the number of syncytiotrophoblasts in these clumps was markedly reduced on GD 13, and the gap between the two GLUT1-positive lines expanded remarkably in the trophoblastic septa, with reduced cell density on GD 15 (Fig. 4e). There was a decrease in the number of phospho-histone H3-positive cells on GDs 13 and 15 in the CPA GD 12-treated group and on GDs 15 and 17 in the CPA GD 14-treated group (Fig. 6).

Basal zone

The thickness of the basal zone decreased on GD 15 in the CPA-treated groups, and then increased from GD 17 onwards in the CPA GD 12-treated group and on GD 17 in the CPA GD 14-treated group (Fig. 3). Apoptosis of spongiotrophoblasts was detected, and the number of TUNEL-positive cells increased on GDs 13 and 15 in the CPA GD 12-treated group and on GD 15 in the CPA GD 14-treated group (Figs. 4b and 5). In the CPA GD 12-treated group, there were enlargement of spongiotrophoblast, increased trophoblastic giant cells, and decreased glycogen cell islands on GD 15, compared to those in the control group (Fig. 4f and 4g). After GD 17 when the fetuses died, the spongiotrophoblasts remained without regression. However, some of these trophoblasts showed hyaline droplet degeneration, and cystic degeneration of glycogen cells containing blood was scattered (Fig. 4f). In the CPA GD 14-treated group, there was a slight decrease in glycogen cell islands on GD 15 (Fig. 4g), as well as cystic degeneration of glycogen cells from GD 17 onwards. In all groups, there was no change in the number of phospho-histone H3-positive cells (Fig. 6). GLUT1 expression was detected along the rim of spongiotrophoblasts from GD 13 onwards, and then increased with placental development.

Decidua basalis

In the CPA GD 12-treated group, the thickness of the decidua basalis increased from GD 13 onwards (Fig. 3). From GD 15 onwards, edema and hemorrhages were observed, and necrosis progressed in a wedge-shaped crack

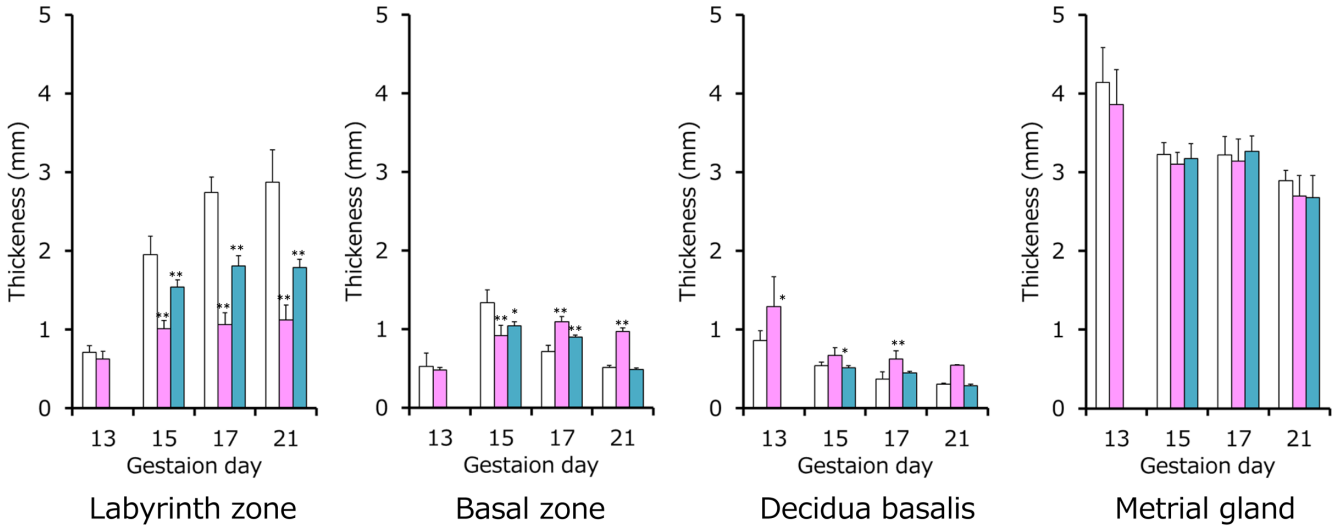

Fig. 3. Thickness of the labyrinth zone, basal zone, decidua basalis, and metrial gland. White, control; pink, cyclophosphamide (CPA) gestation day (GD) 12-treated group; blue, CPA GD 14-treated group. Each value represents mean ± standard deviation. *, ** Significantly different from control at $p<0.05$ and $p<0.01$, respectively (Student's t-test, Dunnett's test).

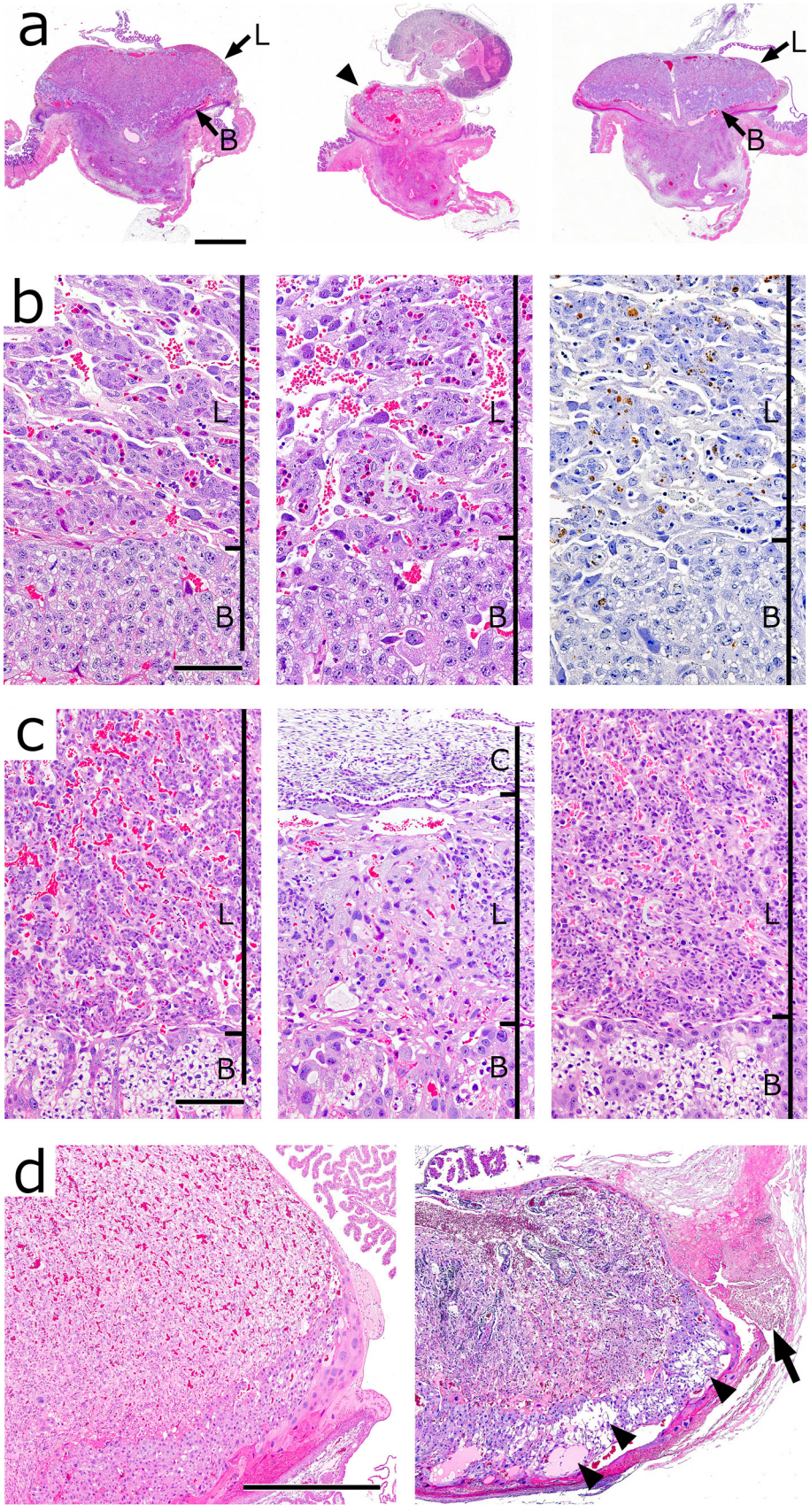

Fig. 4.

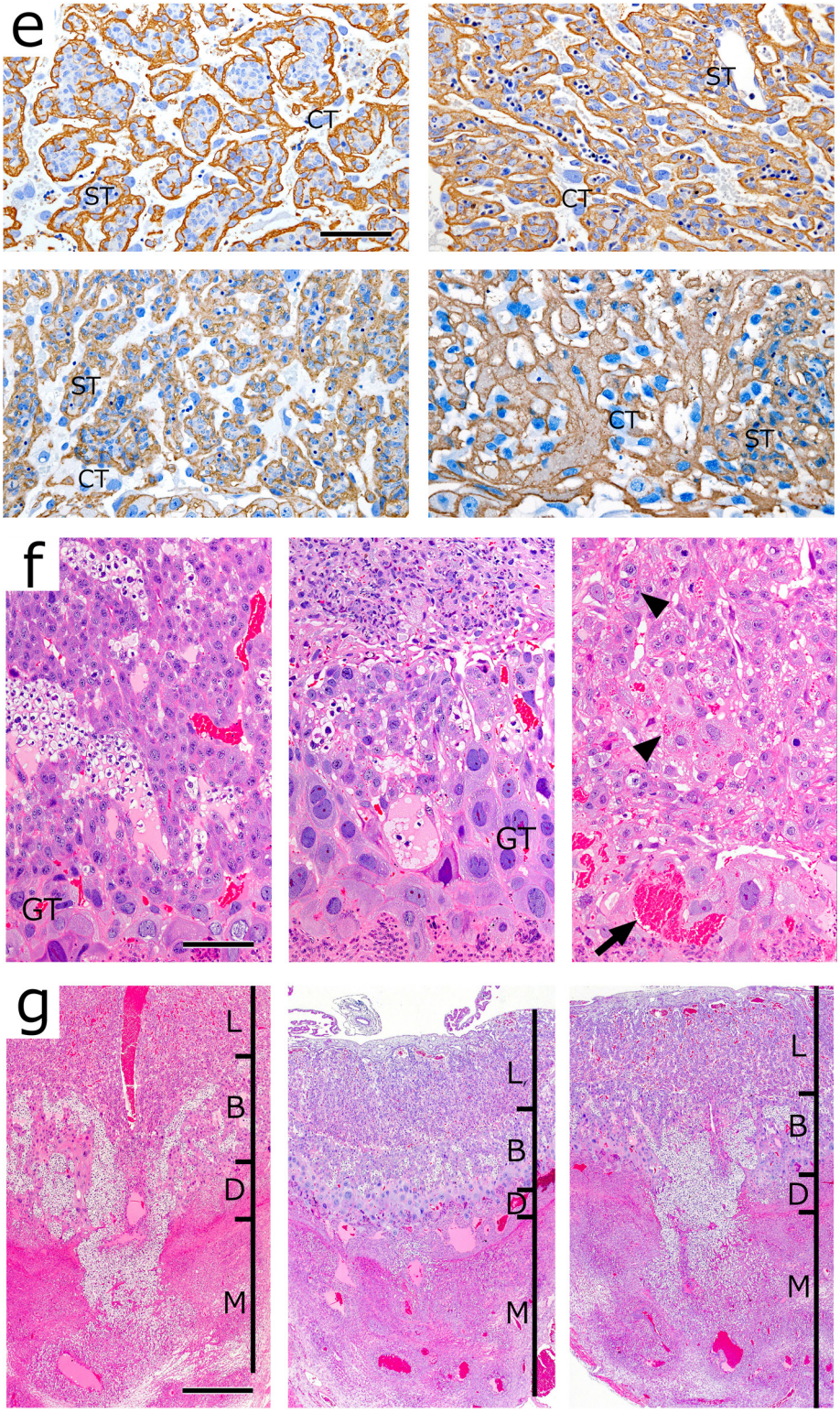

Fig. 4.

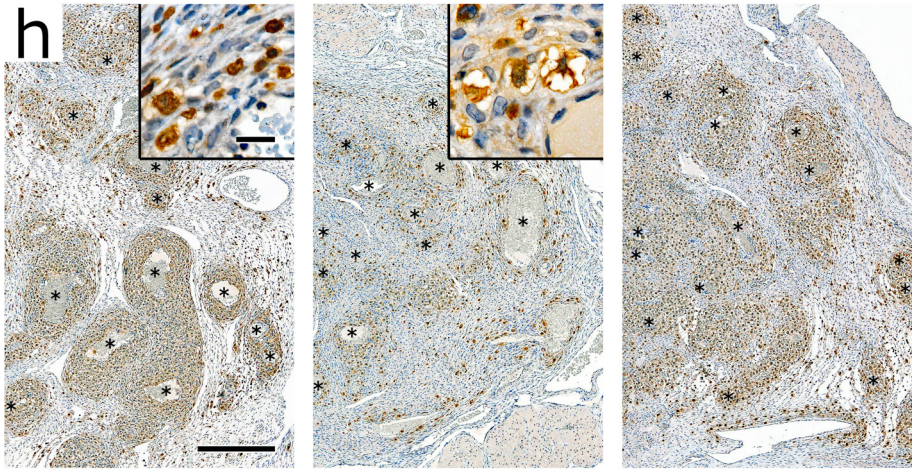

Fig. 4. Histopathological placenta findings. **a.** Low magnification images of placenta on gestation day (GD) 17. Disruption of the fetal part of the placenta (▲) in the cyclophosphamide (CPA) GD 12-treated group. Small placenta with thinning of the labyrinth zone and thickening of the basal zone in CPA GD 14-treated groups. Left, control group; middle, CPA GD 12-treated group; right, CPA GD 14-treated group. Hematoxylin and eosin (HE) staining. Bar, 2,000 µm. **b.** Apoptosis in the labyrinth and basal zones on GD 13. Apoptosis of trophoblasts in the labyrinth zone and spongiotrophoblasts in the basal zone in the CPA-GD 12-treated group. Left, control group. HE staining, middle, CPA GD 12-treated group. HE staining, right, CPA GD 12-treated group. TdT-mediated dUTP nick end labeling (TUNEL) method stain. Bar, 100 µm. **c.** Damaged trophoblasts in the labyrinth zone and basal zone on GD 15. Focal thickened trophoblastic septum with prominent cytotrophoblasts and reduction in syncytiotrophoblasts in the CPA-treated groups. In the CPA GD 12-treated group, chorionic plate thickening, decreased glycogen cells, and larger spongiotrophoblasts in the basal zone. Left, control group, middle, CPA GD 12-treated group; right, CPA GD 14-treated group. HE stain. Bar, 100 µm. **d.** Degenerated changes in the labyrinth zone, basal zone, and decidua basalis on GD 17. Diffuse calcification and thrombosis in the labyrinth zone. Cystic degeneration of glycogen cells (arrowhead). Increased cellular debris mass derived from the decidua basalis at the edge of the placenta (arrow). Left, control group; right, CPA GD 14-treated group. HE stain. Bar, 500 µm. **e.** Glucose transporter 1 (GLUT1) of trophoblastic septa on GDs 13 and 15. Decreased number of syncytiotrophoblasts in clumps surrounded by GLUT1 lines on GD 13 and a remarkably expanded gap between two GLUT1 expression lines in the trophoblastic septa with prominent cytotrophoblasts on GD 15 in the CPA GD 12-treated group. Upper, GD 13; lower, GD 15; right, control group; left, CPA GD 12-treated group. GLUT1 immunohistochemistry stain. Bar, 100 µm. **f.** Degenerated changes of trophoblasts in the basal zone on GDs 15 and 17. Increased trophoblastic giant cells (GT), spongiotrophoblast enlargement, and decreased glycogen cell islands on GD 15. Hyaline droplet degeneration (arrowhead) and cystic degeneration of glycogen cells containing blood (arrow) on GD 17. Left, control group on GD 15; middle, CPA GD 12-treated group on GD 15; right, CPA GD 12-treated group on GD 17. HE stain. Bar, 100 µm. **g.** Invading glycogen cells into the metrial gland on GD 15. Decreased glycogen cells in the basal zone of the CPA-treated groups. Prominent GTs and invasion of few interstitial trophoblasts from the basal zone into the metrial gland in the CPA GD 12-treated group. Left, control group; middle, CPA GD 12-treated group; right, CPA GD 14-treated group. HE stain. Bar, 500 µm. **h.** Decreased uterine natural killer (uNK) cells in the metrial gland on GD 15. Decreased perforin-positive cells, uNK cells around the spiral arteries (*) in the CPA GD 12-treated group. Insert: uNK cells showing swelling and vacuolar degeneration. Left, control group; middle, CPA GD 12-treated group; right, CPA GD 14-treated group. Perforin immunohistochemical staining. Bar, 250 µm/insert bar, and 20 µm, respectively. L: labyrinth zone; B: basal zone; D: decidua basalis; M: metrial gland; C: chorionic plate; CT: cytotrophoblast; GT: trophoblastic giant cell; ST: syncytiotrophoblast.

from the margins to the center. On GD 21, the fetal part of the placenta was detached from the decidua basalis, and the surface of the decidua basalis was covered with endometrial epithelia in some placentas. In the CPA GD 14-treated group, a cell debris mass derived from the decidua basalis was detected at the edge of the placenta from GD 17 onwards, which corresponded to the white peripheral rim that was observed macroscopically (Figs. 2a and 4d). In all groups, GLUT1 expression was slightly scattered in the decidua cells just beneath the basal zone, but only on GD 13.

Metrial gland

There were no differences in the thickness of the metrial gland between the control and CPA-treated groups (Fig. 3). The number of perforin-positive cells, considered uNK cells, around the spiral arteries decreased from GD 13 to GD 17 in the CPA GD 12-treated group and on GD 17 in the CPA GD 14-treated group (Figs. 4h and 7). uNK cells showing swelling and vacuolar degeneration were scattered in the CPA-treated groups (Fig. 4h). The number of phospho-histone H3-positive cells decreased from GD 13 to GD 17 in the CPA GD 12-treated group and from GD 15 to GD 17 in the CPA GD 14-treated group (Fig. 6). In the CPA GD 12-treated group, the number of TUNEL-positive cells increased on GD 13 (Fig. 5), and a small number of interstitial trophoblasts invaded the metrial gland from the basal zone on GD 15 (Fig. 4g). In all groups, GLUT1 expression was detected in some endometrial stromal cells from GD 13 onwards and in interstitial trophoblasts on GDs 15 and 17.

Yolk sac

Apoptosis of the epithelium was detected, and the num-

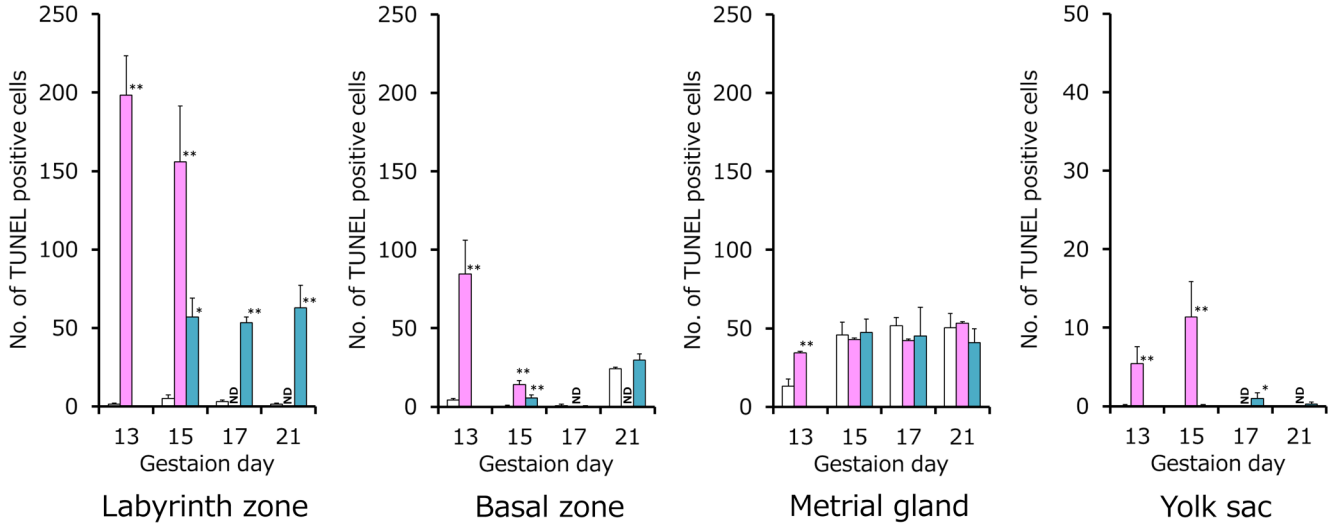

Fig. 5. Number of TdT-mediated dUTP nick end labeling (TUNEL)-positive cells. Each value represents mean ± standard deviations. *, ** Significantly different from control at $p<0.05$ and $p<0.01$, respectively (Student's t-test/Welch's t-test and Dunnett's test). ND: not done. White, control group; pink, cyclophosphamide (CPA) gestation day (GD) 12-treated group; blue, CPA GD 14-treated group.

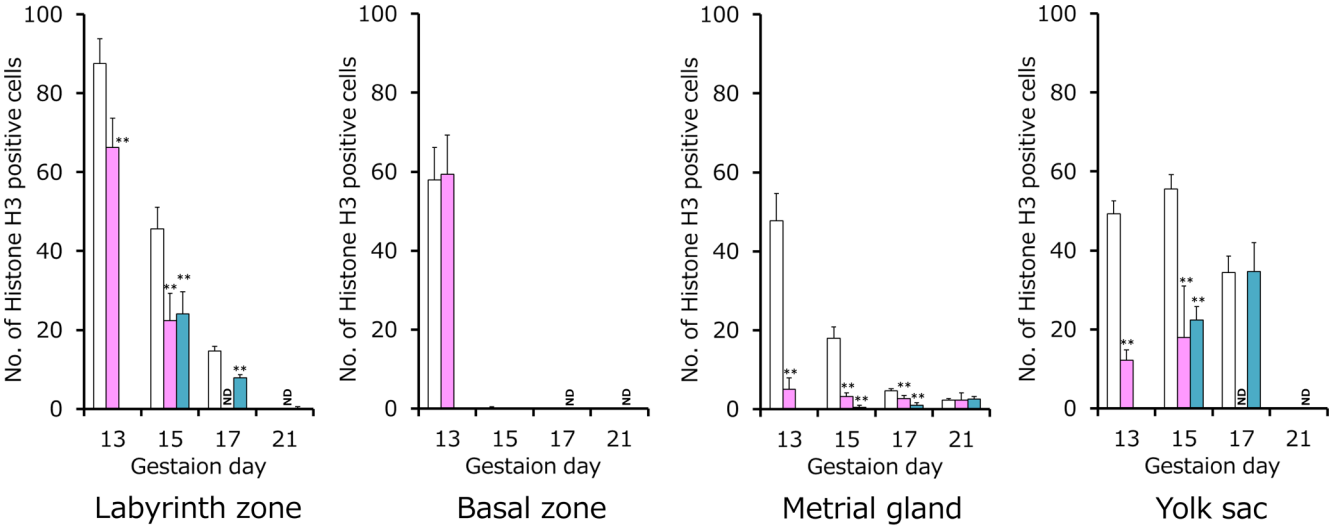

Fig. 6. Number of phospho-histone H3-positive cells. Each value represents mean ± standard deviations. *, ** Significantly different from control at $p<0.05$ and $p<0.01$, respectively (Student's t-test/Welch's t-test and Dunnett's test). ND, not done. White, control group; pink, cyclophosphamide (CPA) gestation day (GD) 12-treated group; blue, CPA GD 14-treated group.

ber of TUNEL-positive cells increased on GDs 13 and 15 in the CPA GD 12-treated group and on GD 17 in the CPA GD 14-treated group (Fig. 5). The number of phospho-histone H3-positive cells decreased on GDs 13 and 15 in the CPA GD 12-treated group and on GD 15 in the CPA GD 14-treated group (Fig. 6). In all groups, GLUT1 expression was detected in the epithelium on GD 13, and then decreased and disappeared by GD 17.

Discussion

In developing placentas, mitosis and apoptosis play important roles in regulating the number of placental cells. Particularly, apoptosis in the placenta is a normal constituent of trophoblast turnover for differentiation during placental development[15]. However, apoptosis is also induced by various undesirable exogenous stimuli, such as preeclampsia, hypoxia, and cytotoxic agents[16]. CPA-induced fetal and placental toxicity is related to apoptosis via molecules such as Bax, p65, and IκBα, mediated by phosphoramide mustard,

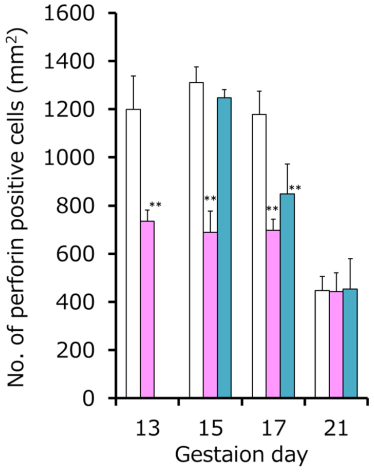

Fig. 7. Number of perforin-positive cells in the metrial gland. Each value represents mean ± standard deviations. ** Significantly different from control at $p<0.01$ (Student's t-test and Dunnett's test). White, control group; pink, cyclophosphamide (CPA) gestation day (GD) 12-treated group; blue, CPA GD 14-treated group.

an activated metabolite of CPA[17, 18]. In the present study, apoptosis and/or cell proliferation inhibition was observed in the labyrinth, basal and metrial gland, and yolk sac as CPA-induced placental toxicity. In particular, the placental lesions due to CPA-induced apoptosis were most prominent in the labyrinth zone, which has high cell proliferation activity.

In the labyrinth zone, the trophoblastic septa are histologically composed of one cytotrophoblast layer, two syncytiotrophoblast layers (I and II), and fetal vessels in rodents[19]. The two syncytiotrophoblast layers are closely apposed and form a placental barrier. GLUT1, a facilitated-diffusion glucose transporter isoform, is localized on the membrane of syncytiotrophoblast layer I facing the maternal blood side and on the membrane of syncytiotrophoblast layer II facing the fetal vessels[20]. Thus, GLUT1 immunohistochemistry is considered a suitable marker for detecting placental barrier thickness. In the present study, the data revealed that the most distinctive changes in CPA exposure were selective syncytiotrophoblast apoptosis and an expanded gap between the two GLUT1-positive lines in the trophoblastic septa. These changes suggest that a small number of residual syncytiotrophoblasts are swollen to compensate for the decreased cell density of the trophoblastic septa and ensure that the placental barrier is barely maintained. In the CPA GD 12-treated group, the lesions in the trophoblastic septa were more pronounced, as clumps composed of many immature syncytiotrophoblasts were lost, compared to the CPA GD 14-treated group. However, it was unclear whether the fetal death in the CPA GD 12-treated group was due to the direct effect of CPA or to the disruption of the damaged trophoblastic septa. On the other hand, there are known differences in the sensitivity between syncytiotrophoblasts and cytotrophoblasts, depending on the toxicant. In *in vitro* human trophoblasts, the apoptotic sensitivity of cytotrophoblasts to some toxicants is higher than that of syncytiotrophoblasts[21]. Conversely, syncytiotrophoblasts are more sensitive than cytotrophoblasts in cadmium-exposed rat placentas[22]. In rodents, cytotrophoblasts play a role in slowing maternal blood flow, whereas syncytiotrophoblasts are major components of the placental barrier. Thus, syncytiotrophoblasts are certainly exposed to substances that penetrate the placental barrier and reach the fetus. In the present study, it is likely that syncytiotrophoblasts were highly sensitive to CPA.

The basal zone is fully developed on GD 15, gradually leading to regression before parturition during normal development[2]. The basal zone comprises spongiotrophoblasts, glycogen cells, and trophoblastic giant cells. Glycogen cells are derived from spongiotrophoblasts, and then differentiate into interstitial trophoblasts on GD 15, which invade the metrial gland[23]. In addition, placental glycogen has been suggested to represent a source of readily mobilized glucose, which is required during periods of high fetal demand[24]. In the present study, the basal zone on GD15 in the CPA-treated groups showed thinning with hypoplasia of glycogen cell islands due to a reduction in spongiotrophoblasts via apoptosis. In addition, hypoplasia of glycogen cell islets induced an inhibition of interstitial trophoblast invasion into the metrial gland. Therefore, CPA induced apoptosis not only in syncytiotrophoblasts, but also in spongiotrophoblasts, thereby resulting in a delay in basal zone development. Hypoplasia of glycogen cell islands may be one of the factors contributing to CPA-induced IUGR.

Macroscopically, the placenta on GDs 17 and 21 in the CPA GD 14-treated group showed a white peripheral rim, which was histopathologically composed of a cellular debris mass derived from the decidua basalis. Similar changes have also been reported in small placentas induced by cisplatin[4], 6-mercaptopurine[25], and busulfan[26], among others. Thus, this lesion is considered a non-specific change in small placentas. It is speculated that the peripheral regions of the decidua basalis cannot contact the basal zone because of insufficient development of the fetal part of the placenta, which then leads to necrosis, resulting in a white peripheral rim.

The metrial gland is composed of uNK cells, decidualized endometrial stromal cells, invading trophoblasts (interstitial and endovascular), and spiral arteries, among others[2]. As fetal development progresses, spiral arteries are remodeled to ensure sufficient delivery of maternal blood to the developing fetus[27]. The uNK cells contribute to spiral artery remodeling[28], which begins from GD 10[29]. Consistent with this, the number of uNK-cells increases from GD 10, reaches a maximum on GDs 14 or 15, and then decreases via apoptosis[30]. For tamoxifen[31] and estrogen[32], administration before GD 12 induces metrial gland hypoplasia, which is closely involved in hypoplastic spiral arteries with a decrease in uNK cells[33]. In the present study, although the administration of CPA on GD 12 induced a decrease in uNK cells and an inhibition of interstitial trophoblast invasion in

the metrial gland, there were no effects on spiral arterial remodeling or metrial gland development. In addition, after fetal death, the collapsed fetal part of the placenta gradually separated from the decidua basalis and was then absorbed, whereas there were no marked histopathological changes in the metrial gland. Thus, the critical period for metrial gland formation, including spiral arterial remodeling, is prior to GD 12, and the inhibition of interstitial trophoblast invasion has minimal effect on metrial hypoplasia. The metrial gland remained without regression after fetal death or resorption once it had formed.

The visceral yolk sac is involved in the placental functions until just before parturition in rodents and rabbits, as the inverted yolk sac placenta[2, 33]. CPA inhibits the absorptive activity of the endoderm of the visceral layer of the yolk sac placenta, which may lead to quantitative and/or qualitative nutritional changes in the developing embryos of rabbits[34]. In contrast, in rat embryo culture, phosphoramide mustard is reported to induce DNA fragmentation in the embryos but not in the yolk sac[35]. In this study, CPA induced apoptosis and inhibited cell proliferation in the yolk sac. However, the degree of apoptosis was minor in the yolk sac relative to that in other parts of the placenta in the CPA-treated groups, even though cell proliferative activity in the yolk sac is generally as high as that in the labyrinth zone during normal placental development. In addition, there is a low incidence of apoptosis in the yolk sacs of dibutyltin-exposed[35] and β-naphthoflavone-exposed[36] pregnant rats, compared to other parts of the placenta. In mouse embryo cultures, the cells of the extraembryonic yolk sac derived from GD 8.5 embryos are substantially more resistant to teratogen-induced activation of the mitochondrial apoptotic pathway and subsequent apoptosis, compared to other embryonic tissues[37]. This suggests that the susceptibility of toxicants to apoptosis is generally lower in the yolk sac than in other fetal parts of the placenta in rodents.

In conclusion, the most distinctive change due to CPA exposure on GD 12 or 14 was selective syncytiotrophoblast apoptosis in the labyrinth zone, resulting in a small placenta. The severity of these lesions was higher in the CPA GD 12-treated group than in the CPA GD 14-treated group. In the metrial gland, CPA exposure on GD 12 induced a decrease in uNK cells caused by apoptosis and/or cell proliferation inhibition, but did not affect metrial gland development.

Disclosure of Potential Conflicts of Interest: The authors have no conflicts of interest to declare.

Acknowledgements: The authors thank Ms. Yukiko Sudo, Ms. Kaori Maejima, Ms. Hiromi Asako, Mr. Atsushi Funakoshi, Mr. Makoto Tsuchiya, and Mr. Yoshinori Tanaka for their excellent technical assistance.

References

1. Battaglia FC, and Meschia G. Fetal and placental growth. In: An introduction to fetal physiology, 1st ed. FC Battaglia, and G Meschia (eds). Academic Press, Orlando. 1–27. 1986.
2. Furukawa S, Tsuji N, and Sugiyama A. Morphology and physiology of rat placenta for toxicological evaluation. J Toxicol Pathol. **32**: 1–17. 2019. [Medline] [CrossRef]
3. Furukawa S, Hayashi S, Usuda K, Abe M, and Ogawa I. The relationship between fetal growth restriction and small placenta in 6-mercaptopurine exposed rat. Exp Toxicol Pathol. **63**: 89–95. 2011. [Medline] [CrossRef]
4. Furukawa S, Hayashi S, Usuda K, Abe M, Hagio S, and Ogawa I. Effect of cisplatin on rat placenta development. Exp Toxicol Pathol. **65**: 211–217. 2013. [Medline] [CrossRef]
5. Chen B, Cyr DG, and Hales BF. Role of apoptosis in mediating phosphoramide mustard-induced rat embryo malformations in vitro. Teratology. **50**: 1–12. 1994. [Medline] [CrossRef]
6. Matalon ST, Ornoy A, and Lishner M. Review of the potential effects of three commonly used antineoplastic and immunosuppressive drugs (cyclophosphamide, azathioprine, doxorubicin on the embryo and placenta). Reprod Toxicol. **18**: 219–230. 2004. [Medline] [CrossRef]
7. Singh G, Sinha N, Koushik C J, Mathur SK, and Srivastava S. Detecting role of apoptosis in mediating cyclophosphamide induced teratogenesis in vitro. Toxicol Mech Methods. **15**: 391–397. 2005. [Medline] [CrossRef]
8. Rengasamy P. Congenital malformations attributed to prenatal exposure to cyclophosphamide. Anticancer Agents Med Chem. **17**: 1211–1227. 2017. [Medline] [CrossRef]
9. Mirkes PE. Cyclophosphamide teratogenesis: a review. Teratog Carcinog Mutagen. **5**: 75–88. 1985. [Medline] [CrossRef]
10. Padmanabhan R, and Singh S. Histopathological changes of placenta induced by cyclophosphamide in mice. Cong Anom. **20**: 365–373. 1980.
11. Padmanabhan R, and Singh S. Histopathological changes of placenta induced by cyclophosphamide in rats. Cong Anom. **24**: 1–8. 1984. [CrossRef]
12. Ashby R, Davis L, Dewhurst BB, Espinal R, Penn RN, and Upshall DG. Aspects of the teratology of cyclophosphamide (NSC-26271). Cancer Treat Rep. **60**: 477–482. 1976. [Medline]
13. Engelbregt MJ, van Weissenbruch MM, Popp-Snijders C, Lips P, and Delemarre-van de Waal HA. Body mass index, body composition, and leptin at onset of puberty in male and female rats after intrauterine growth retardation and after early postnatal food restriction. Pediatr Res. **50**: 474–478. 2001. [Medline] [CrossRef]
14. Moroki T, Matsuo S, Hatakeyama H, Hayashi S, Matsumoto I, Suzuki S, Kotera T, Kumagai K, and Ozaki K. Databases for technical aspects of immunohistochemistry: 2021 update. J Toxicol Pathol. **34**: 161–180. 2021. [Medline] [CrossRef]
15. Huppertz B, and Kingdom JC. Apoptosis in the trophoblast—role of apoptosis in placental morphogenesis. J Soc Gynecol Investig. **11**: 353–362. 2004. [Medline] [CrossRef]
16. Levy R. The role of apoptosis in preeclampsia. Isr Med Assoc J. **7**: 178–181. 2005. [Medline]
17. Mammon K, Savion S, Keshet R, Aroch I, Orenstein H,

Fein A, Torchinsky A, and Toder V. Expression of apoptosis-associated molecules in the fetoplacental unit of cyclophosphamide-treated mice. Reprod Toxicol. **22**: 774–782. 2006. [Medline] [CrossRef]
18. Torchinsky A, Savion S, Gorivodsky M, Shepshelovich J, Zaslavsky Z, Fein A, and Toder V. Cyclophosphamide-induced teratogenesis in ICR mice: the role of apoptosis. Teratog Carcinog Mutagen. **15**: 179–190. 1995. [Medline] [CrossRef]
19. Elmore SA, Cochran RZ, Bolon B, Lubeck B, Mahler B, Sabio D, and Ward JM. Histology atlas of the developing mouse placenta. Toxicol Pathol. **50**: 60–117. 2022. [Medline] [CrossRef]
20. Shin BC, Fujikura K, Suzuki T, Tanaka S, and Takata K. Glucose transporter GLUT3 in the rat placental barrier: a possible machinery for the transplacental transfer of glucose. Endocrinology. **138**: 3997–4004. 1997. [Medline] [CrossRef]
21. Crocker IP, Barratt S, Kaur M, and Baker PN. The in-vitro characterization of induced apoptosis in placental cytotrophoblasts and syncytiotrophoblasts. Placenta. **22**: 822–830. 2001. [Medline] [CrossRef]
22. Yamagishi Y, Furukawa S, Tanaka A, Kobayashi Y, and Sugiyama A. Histopathological localization of cadmium in rat placenta by LA-ICP-MS analysis. J Toxicol Pathol. **29**: 279–283. 2016. [Medline] [CrossRef]
23. Lutton EJ, Lammers WJEP, James S, van den Berg HA, and Blanks AM. Identification of uterine pacemaker regions at the myometrial-placental interface in the rat. J Physiol. **596**: 2841–2852. 2018. [Medline] [CrossRef]
24. Tunster SJ, Watson ED, Fowden AL, and Burton GJ. Placental glycogen stores and fetal growth: insights from genetic mouse models. Reproduction. **159**: R213–R235. 2020. [Medline] [CrossRef]
25. Furukawa S, Usuda K, Abe M, Hayashi S, and Ogawa I. Effect of 6-mercaptopurine on rat placenta. J Vet Med Sci. **70**: 551–556. 2008. [Medline] [CrossRef]
26. Furukawa S, Usuda K, Abe M, Hayashi S, and Ogawa I. Busulfan-induced apoptosis in rat placenta. Exp Toxicol Pathol. **59**: 97–103. 2007. [Medline] [CrossRef]
27. Shukla V, and Soares MJ. Modeling trophoblast cell-guided uterine spiral artery transformation in the rat. Int J Mol Sci. **23**: 2947. 2022. [Medline] [CrossRef]
28. Renaud SJ, Scott RL, Chakraborty D, Rumi MA, and Soares MJ. Natural killer-cell deficiency alters placental development in rats. Biol Reprod. **96**: 145–158. 2017. [Medline] [CrossRef]
29. Picut CA, Swanson CL, Parker RF, Scully KL, and Parker GA. The metrial gland in the rat and its similarities to granular cell tumors. Toxicol Pathol. **37**: 474–480. 2009. [Medline] [CrossRef]
30. Peel S. Granulated Metrial Gland Cells. Advances in Anatomy Embryology and Cell Biology. Springer-Verlag, Berlin. 1989.
31. Furukawa S, Hayashi S, Usuda K, Abe M, and Ogawa I. The impairment of metrial gland development in tamoxifen exposed rats. Exp Toxicol Pathol. **64**: 121–126. 2012. [Medline] [CrossRef]
32. Furukawa S, Hayashi S, Usuda K, Abe M, Hagio S, Kuroda Y, and Ogawa I. Effect of estrogen on rat placental development depending on gestation stage. Exp Toxicol Pathol. **65**: 695–702. 2013. [Medline] [CrossRef]
33. Furukawa S, Hayashi S, Usuda K, Abe M, Hagio S, and Ogawa I. Toxicological pathology in the rat placenta. J Toxicol Pathol. **24**: 95–111. 2011. [Medline] [CrossRef]
34. Claussen U, Hettwer H, Voelcker G, Krengel HG, and Servos G. The embryotoxicity of cyclophosphamide in rabbits during the histiotrophic phase of nutrition. Teratog Carcinog Mutagen. **5**: 89–100. 1985. [Medline] [CrossRef]
35. Furukawa S, Tsuji N, Kobayashi Y, Yamagishi Y, Hayashi S, Abe M, Kuroda Y, Kimura M, Hayakawa C, and Sugiyama A. Effect of dibutyltin on placental and fetal toxicity in rat. J Toxicol Sci. **42**: 741–753. 2017. [Medline] [CrossRef]
36. Furukawa S, Tsuji N, Hayashi S, Kuroda Y, Kimura M, Hayakawa C, Takeuchi K, and Sugiyama A. The effects of β-naphthoflavone on rat placental development. J Toxicol Pathol. **32**: 275–282. 2019. [Medline] [CrossRef]
37. Soleman D, Cornel L, Little SA, and Mirkes PE. Teratogen-induced activation of the mitochondrial apoptotic pathway in the yolk sac of day 9 mouse embryos. Birth Defects Res A Clin Mol Teratol. **67**: 98–107. 2003. [Medline] [CrossRef]